Supplementary Information

Supplementary Experimental Procedures

Construction of bubble stimuli: Bubbles stimuli were constructed as described previously (Gosselin and Schyns, 2001). Briefly, one of 8 face base images (chosen from the Ekman and Friesen stimulus set, 4 different individuals (2 female and 2 male) showing happy and fearful expressions each, all normalized for mean luminance, contrast, and position of eyes and mouth) and their mirror images were sparsely sampled only in the 2-D face plane (no spatial frequency sampling was done) and presented to participants one at a time. The number of bubbles shown was adapted continuously using the QUEST-staircase method with β=3.5, δ=0.01 and γ=0.5 (Watson and Pelli, 1983) targeting an error rate of 20% (the error trials were used to compute the classification image, see below). The mean asymptotic performance actually obtained was 82.6%, confirming the validity of the adaptive procedure. The location of each bubble was chosen randomly and independently of all other bubbles. As subjects improved, the number of bubbles required decreased (learning curve, Fig 2c). The same 8 faces were also used for the whole face and eye/mouth region trials. Patients performed a short test version of the task (data not shown or analyzed) immediately prior to the experiment with the same stimuli. We implemented the task with the Psychophysics Toolbox in MATLAB (Brainard, 1997).

Electrode localization from structural MRIs: To identify electrode recording sites in the amygdala, T2 relaxation times were measured using spin-echo dual-echo sequences on a 1.5-T Toshiba MR scanner. 25 contiguous axial slices were acquired (0.575 x 0.575 mm in-plane, 5 mm thick, TR=5777.5 ms, TE=105 ms, flip angle = 90°). The imaging slices covered the entire brain, including the amygdala. The electrodes were clearly visible as dark lines in the T2 scans. Images were subsequently processed using SPM8 (Friston, 2007). Scans were first segmented and normalized to the standard MNI space. The electrode tip coordinates were visualized and manually labeled in FSL (Jenkinson et al., 2012). A mask was created in MATLAB for each patient with each recording site as a 3 x 3 x 3 mm cube centering on the identified electrode tip. All masks were then overlaid on the standard MNI152 template with 1 mm isotropic resolution.

Each color in Supplementary Figure S1 denotes the bilateral recording sites for an individual patient.

Data analysis: Spike waveforms. Comparisons of the waveform of different neurons were made based on the through-to-peak time of the mean waveform (Mitchell et al., 2007). The mean waveform is the average of all spikes assigned to the cluster (see Fig. 2 for examples). The polarity of the mean waveforms was inverted if necessary such that the through always occurs before the peak. We also verified whether there is a correlation between the through-to-peak time and the mean firing rate of a unit. For this, the mean firing rate was defined as the mean rate over the entire duration of 3.5s of all valid trials.

Data analysis: whole-face selective cells. We selected and quantified whole-face selective cells as described previously (Rutishauser et al., 2011). Briefly, cells were considered as whole-face selective if their firing rate after stimulus onset differed significantly between trials showing whole faces and parts (ROIs). We further quantified the whole-face selectivity of each unit using the whole-face index (WFI). The WFI of unit i is the baseline normalized difference in mean response to whole faces trials compared to bubbles trials (Eq S1).

$$WFI_i = \frac{\overline{R}_{WholeFace} - \overline{R}_{Bubbles}}{\overline{R}_{Baseline}} 100\% \qquad \text{(Eq S1)}$$

If the WFI is different from 0, the unit responds to whole-faces differently than to partially revealed faces. Note that a large nonzero WFI, regardless whether negative or positive, indicates whole-face-selective responses. Thus we used the absolute value of the WFI throughout this paper. Also note that the WFI and the selection of the cells as whole face selective is statistically independent: selection is comparing whole-face trials with parts trial (ROIs) whereas the WFI is based on the difference between whole-face trials and bubbles trials.

Data analysis: Correlation of behavioral and neuronal classification images.

We assessed the correlation between individual NCIs with an average group behavioral classification image. The group behavioral classification image (GBCI) was the average of a total of 9 control subjects that were not used for the neuronal analysis (n=6 nonsurgical control

subjects that did not have ASD, also used for eye tracking, and the 3 surgical non-ASD subjects that did not yield any neuronal data) and thus originated from a group of subjects independent of those who contributed the neuronal recordings. For each unit j with a significant NCI, we calculated and appropriately normalized the 2D correlation between the NCI and the GBCI (Eq S2).

$$CIcorr_j(x,y) = NCI(x,y) * GBCI(x,y) \qquad \text{(Eq S2)}$$

Both the NCI and the GBCI are in terms of z-scores. The distribution of the product of two z-scores, however, is not well defined and we thus estimated this distribution empirically using a bootstrap procedure (as described above). This procedure yielded an estimate of the mean μ_j and variance σ_j of CIcorr at every pixel (x,y). The z-scored 2D correlation (as shown in Fig. 6a,b) is

$$Z\_CIcorr_j(x,y) = \frac{CIcorr_j(x,y) - \mu_j(x,y)}{\sigma_j(x,y)} \qquad \text{(Eq S3)}$$

Data analysis: interspike intervals analysis. We computed the interspike interval distribution (ISI) of each cell by considering all spikes fired during the experiment and quantified it using two metrics: the modified coefficient-of-variation C_{V2} and the burst index (BI). The BI was defined as the proportion of ISIs less than 10ms (Wyler et al., 1975). The CV2 (Eq S4) is a function of the difference between two adjacent ISIs and is a standard measure to quantify spike-train variability that is robust to underlying rate changes (Holt et al., 1996). In contrast, the coefficient-of-variation measure CV is only valid for stationary processes, i.e. fixed mean rate and is thus not applicable for this analysis.

$$CV2 = \frac{1}{N}\sum_{i=1}^{N}\frac{2|ISI_{i+1} - ISI_i|}{ISI_{i+1} + ISI_i} \qquad \text{(Eq S4)}$$

Data analysis: variability of responses. We quantified the variability of the spiking response that followed the onset of the face on the screen using the coefficient of variation (standard deviation divided by mean) of the number of spikes counted in the same window (1.5s) as used to quantify the NCIs. For each cell, we computed the CV of its response for either all trials, only WF trials, or only bubble trials and then compared the CV values of different groups of neurons. CV values were approximately 1 as expected and there were no significant

differences between the CV values of neurons from ASD and controls for all cells, only cells with NCIs, or only WF cells either for all trials, only bubble trials or only WF trials.

Data analysis: Exclusion of epileptic areas. To check that results were not influenced by abnormal responses within regions of seizure focus (Rutishauser, 2008), we repeated analyses by conservatively excluding all units originating from the brain hemisphere in which the temporal epileptic seizure focus was detected (if there was one; see Table S1). 121 units remained, 76 of which had mean firing rates>0.5Hz. 21 of these (28%) of these had significant NCIs (12 of which in the two patients with ASD), which is a very similar proportion compared to when using all cells (29%). Only 5 NCIs were dropped. All results remained quantitatively similar when excluding these NCIs from the analysis. Also note that with one exception, no patient had a seizure origin in the amygdala.

Statistical verification with bootstrap methods.

We also used a non-parametric bootstrap procedure to estimate the significance of the NCIs and arrived at very similar results compared to the cluster test. The procedure (see below) is more conservative and thus results in fewer cells with significant NCIs (15 instead of the previous 26), but importantly all differences that we report between ASD and controls remain significant and qualitatively similar (average Z-value in mouth and eye ROIs is significantly larger and smaller in ASD compared to controls, respectively, at P=0.003 and P=0.004). The bootstrap procedure was run 200 times for every cell. At each iteration, the order of the noise masks was scrambled randomly such that the association between which noise mask resulted in which spike count was randomized. Thus, the distribution of spike counts observed as well as the distribution of noise masks used was preserved, but their relation was randomized. This yields a reliable estimate of the NCIs to be expected by chance for each cell, taking into account in particular possible effects of unusual noise masks (that arise by chance) or outlier spike responses such as bursts. We then used these random NCIs to estimate the distribution of values at each pixel (x,y) expected by chance and compared it with the value actually observed. The bootstrap test for the significance of NCIs is based on an empirical estimate of the Euler characteristic (EC). The EC quantifies the number of clusters in a thresholded Gaussian random field (Adler, 1981; Worsley, 1994). For example, a EC=2 for a given threshold means that 2

clusters are present for this threshold. The cluster test (see above) is a parametric implementation of this concept (Chauvin et al., 2005; Friston et al., 1993). We also calculated the empirical estimate of the EC (using bootstrap) to further verify our results as follows. For every bootstrapped NCI, we estimated the associated EC for different thresholds T. Then, T was set such that only 5% of randomly permuted trials had an EC>=1. Thus, this procedure assures that the threshold T is fully corrected for multiple comparisons. This empirically estimated threshold T was then used to determine whether an NCI was significant or not.

Data analysis: Comparison between cutout and NCI responses.

We categorized an NCI, regardless of its significance, according to whether it showed a differential response to the mouth, left eye, right eye or neither of those. First, the mean Z-scored NCI within each of the 3 ROIs was calculated and a cell was assigned to one of the groups if the mean Z value within one of the ROIs was >0 whereas it was <0 for the others. 23 of the cells had a mouth NCI, 19 an eye NCI and 49 had neither. For each of the three groups, the average response difference to eye and mouth cutouts was then calculated. For mouth-and eye sensitive cells this quantity was expected to be significantly negative and positive, respectively.

Eye tracking – subjects. We repeated the identical task after patients were released from the hospital at our laboratory at Caltech while tracking eye movements. There were four groups of subjects that performed the task: 1) a control group of non-surgical autism subjects that did not have epilepsy (six subjects, 5 male, mean age 32±12, see Table S2 for autism scores), 2) a control group of matched neurotypical normals (six subjects, 5 male, mean age 25±2), 3) epilepsy subjects without autism from which we also previously recorded neural activity (three subjects, P19,P20 and P21 in Table S1), and 4) the two epilepsy subjects that also had autism. All epilepsy subjects had been operated (partial resection) by the time eye tracking was performed, with the exception of one of the autism subjects with epilepsy (P17). All 17 subjects performed the task under conditions identical to the patients, with the same instructions. Subjects completed between 360-840 trials each (mean 456±176 trials, ±s.d. over subjects). Task performance accuracy as well as the speed of learning during eye tracking were comparable between the non-surgical autism group and the matched neurotypical control group.

There was no significant difference in the number of bubbles reached in the last trial (31.6±25.2 and 17.5±10.3, for controls and ASD, respectively; P=0.28, ±s.d.) as well as the reaction time in bubble trials (866±142ms and 815±179ms; P=0.6, ±s.d.) or all trials (847±122ms and 790±151ms; P=0.49, ±s.d.). This independently confirms our observation on the neurosurgical subjects that showed no difference in performance and reaction time between ASD and control subjects.

Eye tracking was carried out using a non-invasive infrared remote Tobii X300 system together with Tobii Studio 2.2 software. Eye movements were recorded bilaterally with 300 Hz. Stimuli were shown on a 23-inch screen (screen resolution: 1920x1080).

Eye tracking – fixation density analysis. Fixations were detected by a fixation filter in Tobii Studio 2.2 that detects quick changes in the gaze location using a sliding window averaging method (Olsson, 2007). Only correct trials were considered for all fixation density calculations. Fixation locations were smoothed with a 40-pixel 2D Gaussian kernel with a standard deviation of 10 pixels (the same as is used for display of the stimuli and in the analysis throughout). Each heat map indicates the probability of fixating a given location (in arbitrary units), which is calculated based on the number and duration of fixations and which ensured an equal contribution from each subject and statistical independence between subjects.

To correct for possible drift in the calibration of the eye tracker, we performed a post-hoc drift-correction procedure for each trial. Before the presentation of faces, a fixation circle superimposed on a scrambled face image was presented for a random duration between 800 to 1200 ms. We subtracted the mean fixation position of the last 500 ms during this fixation period from all subsequent fixations during the face presentation period.

To quantitatively compare the fixation densities within certain parts of the face, we defined three ROIs: eyes (left and right), mouth and center. Each ROI is a circle with a radius of 35 pixels. The average fixation density within the ROIs was calculated for each subject and category (bubbles, whole faces, parts) during either the entire 500ms post stimulus-onset period or only the last 200ms period before offset of the face. Statistical comparisons were then performed to compare whether the mean fixation density values within the ROIs different between groups (normals, autism subjects without epilepsy, epilepsy patients without autism,

epilepsy patients that had autism; thus there were 4 categories in the subject group variable of the one-way ANOVA).

When counting the number of different fixations subjects made in a particular trial, we started counting at 1. Thus, if subjects made no fixations and stayed at the center, this trial was counted as having 1 fixation.

Eye tracking – conditional probability analysis. For each participant, we computed the conditional probability that, over all correct trials, the participant directed his/her gaze to the revealed parts within the first 500 ms after stimulus onset. In every given trial, each pixel (x,y) was assigned one of three values: 1 if the pixel was revealed and fixated (within 8 pixels, approximately 0.3°), 0 if the pixel was revealed and not fixated, and undefined if the pixel was not revealed. The average conditional probability maps for each patient were calculated by averaging, for each pixel, all the trials where the pixel was revealed. After obtaining such probability maps for each participant, we averaged over participant groups (ASD group and control group).

We computed the average latency of the first fixation to fall into the eye or mouth ROIs (see Figure 5B). For each trial, if there were any fixations falling into an ROI, we took the time that the first fixation entered the ROI as the latency; otherwise, we excluded that trial to compute the average latency. We defined the fastest latency as 3.33 ms (the first sample data point at 300 Hz sampling rate of the eye tracker) if the first fixation of the trial was in an ROI at the beginning of a trial.

Data analysis – selection of bubble trials. We selected trials according to the overlap of the bubbles with the specified eye and mouth ROIs (as shown in Figure 5B). The more overlap between bubbles and ROIs, the more is revealed within the ROI. We chose two categories of ROI trials: those where predominantly only the eye or the mouth was shown. Eye-dominant and mouth-dominant were achieved by enforcing ‘High Eye AND Low Mouth’ overlap and ‘Low Eye AND High Mouth’ overlap, respectively. ‘High’ or ‘Low’ here was above or below the median of the overlapping values across all trials. Selection of trials based

on ROIs revealed was only based on the stimulus shown to the subjects and did not involve the neuronal response or eye movements.

Supplementary Tables

Table S1: Neurosurgical patients: demographics, pathology and neuropsychological evaluation. Abbreviations: Hand: Dominant handedness; Lang Dom: language dominance as determined by Sodium Amybarbital (Wada) test; Benton: Benton Facial Recognition Test, long form score (a measure of ability to discriminate faces visually). Benton scores of 41-54 are in the normal range; WAIS-III: IQ scores from the Wechsler Adult Intelligence Scale: performance IQ (PIQ), verbal IQ (VIQ), full scale IQ (FSIQ), verbal comprehension index (VCI), perceptual organization index (POI). All WAIS-III scores are on average 100 with a s.d. of 15 in the normal population (69 and less falls in the clinically abnormal range, 70-79 borderline, 80-89 low average, 90-109 average, 110-119 high average, 120-129 superior, 130+ very superior). Scores from the Rey-Osterrieth Complex Figures test are raw scores from the subtests copy (visuospatial perception and construction), immediate recall reproduction (IR, additional short-term visual memory demands), and 30-minute delayed recall reproduction (DR, additional longer-term visual memory demands). 36 possible points for each, 18+ is normal depending on age. (*) Are the two neurosurgical autism patients who contributed the single-unit data (see Table S2), (+) are neurosurgical patients without autism who contributed neurons, but had no significant neuronal classification images from our task (NCIs), (++) are neurosurgical patients without autism who contributed neurons that also had significant NCIs and (-) are neurosurgical patients without autism who contributed only behavior (no neurons recorded). Tests indicated with n/a were not performed for clinical reasons.

ID	Age	Sex	Hand	Lang Dom	Epilepsy diagnosis	Benton	WAIS-III					Rey-Osterrieth		
							PIQ	VIQ	FSIQ	VCI	POI	copy	IR	DR
P17 (*)	19	M	R	L	Left inferior frontal	43	128	131	134	122	133	34	23	21
P18 (++)	40	M	R	L	Right mesial temporal hippocampus	52	69	n/a	n/a	n/a	n/a	n/a	n/a	n/a

P19 (++)	34	M	R	n/a	Left supplementary motor neocortex	39	81	74	86	76	80	31	23	20.5
P20 (-)	27	M	R	L	Right mesial temporal hippocampus	49	88	98	81	89	101	33	21	23.5
P21 (-)	20	M	R	n/a	Right dorsolateral neocortex	45	n/a	n/a	n/a	93	89	34	27.5	27
P23 (++)	35	M	R	L	Left mesial temporal amygdala	41	n/a	n/a	n/a	74	86	34	n/a	9.5
P25 (+)	31	M	R	L	Right dorsolateral neocortex	47	81	91	87	98	82	36	9	5
P27 (-)	41	M	R	n/a	Bilateral independent temporal lobe	49	86	91	89	86	88	36	5	5
P28 (*)	23	M	R	L	Right mesial temporal hippocampus	47	79	77	76	78	80	34	9.5	13
P29 (++)	18	F	L	L	Left deep insula	49	104	110	107	107	101	36	19.5	19.5

Table S2: Autism diagnosis for the two neurosurgical patients with ASD (*), and six other (non-neurosurgical) ASD comparison subjects (Autism; not all scores were available for all patients, numbers are stated as mean±s.d. over the number of subjects as indicated in brackets). Both neurosurgical patients met clinical (DSM-IV-TR) and ADOS-criteria for a diagnosis (ASD for P17; Autism for P28). Entries marked with "-" are not available. Abbreviations: Autism Diagnostic Observation Schedule (ADOS), Autism Diagnostic Interview – Revised (ADI-R), Social Responsiveness Scale-2 Adult Form (self report) (SRS-2), Autism Quotient (AQ). ADOS-A Communication; ADOS-B Social Interaction; ADOS-Total Communication + Social; ADOS-D Repetitive and Stereotyped Behavior; ADI-R A Social Interaction; ADI-R B Communication; ADI-R C Stereotyped Behavior.

ID	ADOS Scores				ADI-R Scores			SRS-2	AQ
	A	B	Total	D	A	B	C		
P17*	3	5	8	2	12	8	4	47	25
P28*	6	6	12	0	-	-	-	86	28
Autism	3±1 (6)	7±3 (6)	11±4 (6)	2±2 (6)	23±8 (3)	17±5 (3)	7±3 (3)	85±14 (5)	26±5(5)

Table S3: Number of neurons recorded and analyzed. Left/Right refers to the left and right amygdala, respectively. All is both left and right amygdala.

	# units total			**# units> 0.5 Hz**			**# significant NCIs**		
	Left	Right	All	Left	Right	All	Left	Right	All
ASD	43	13	56	29	8	37	11	5	16
Controls	20	68	88	10	44	54	3	7	10
Total	63	81	144	39	52	91	14	12	26

Table S4: Responses to bubbles. All tests are P<0.05 and independent of one another; that is, a neuron can contribute to more than one of the listed categories. Percentages are out of a total of 91 units. The first two rows are based on all trials, whereas the last three rows are based exclusively on the bubbles trials.

Response Characteristics		**# units**			**% units**
		ASD	Ctrl	All	
Visually responsive (scramble vs. baseline blank screen)		3	10	13	14%
Face responsive (stimulus vs. scramble)		15	27	42	46%
Fear vs. happy (bubbles trials)		3	9	12	13.2%
Identity (1-way ANOVA, 4 identities, bubbles trials)		0	7	7	7.7%
Gender X Fear/Happy (2x2 ANOVA, bubbles trials)	gender ,	1	3	4	4.4%
	fear versus happy	2	10	12	13.2%
	interaction	2	4	6	6.5%

Table S5: Electrophysiological properties of neurons. Numbers shown are calculated based on all spikes during the entire experiment (baseline and stimulus periods). However, quantitatively similar results (with no significant differences) hold when only considering baseline or after-stimulus onset periods (1.5 before or after stim onset). Abbreviations: CV_2 modified coefficient of variation, BI burst index, d peak-to-through distance of waveforms. d values are distributed significantly bimodally, as verified by Hartigan's dip test. Pairwise comparisons between ASD and Ctrl for the three cell groups (all, WF, and NCI, see text for details) are all n.s. with $P>0.05$ (two-tailed t-test for rate, CV2, and BI; and two-tailed Kolmogorov-Smirnov test for d; ± is s.d. over all units as indicated).

	n	**CV2**	**BI**	**d [ms]**
ASD, all	37	0.98±0.06	0.02±0.02	0.65±0.33
Ctrl, all	54	0.97±0.09	0.02±0.02	0.65±0.37
ASD, WF	12	0.93±0.08	0.02±0.02	0.83±0.31
Ctrl, WF	17	0.97±0.06	0.01±0.01	0.63±0.35
ASD, NCI	16	1.00±0.04	0.03±0.02	0.63±0.35
Ctrl, NCI	10	1.05±0.12	0.03±0.02	0.62±0.34

Table S6: Eye movement quantification, as shown in Fig S6. Shown is the average fixation density across subjects, averaged within the ROIs for trials where parts were shown. Abbreviations: Epi = Epilepsy, Ctrl=Control. One-way ANOVAs with factor subject group (ASD, ASD+Epi, Epi, Control) for each ROI were not significant with P>0.05. Paired post-hoc t-tests between ASD and Controls for each ROI and trial type were similarly not significant at P>0.05 (For Parts all 500ms, P=0.61, P=0.12, P=0.97; Parts 200ms only, P=0.88, P=0.09, P=0.94; for central, mouth, eye ROI, respectively; ± shows s.e.m. over subjects, with n as indicated).

	Density central ROI [%]				**Density mouth ROI [%]**				**Density eye ROI [%]**			
Trial Type (n)	**ASD (6)**	**ASD +Epi (2)**	**Epi (3)**	**Ctrl (6)**	**ASD (6)**	**ASD +Epi (2)**	**Epi (3)**	**Ctrl (6)**	**ASD (6)**	**ASD+ Epi (2)**	**Epi (3)**	**Ctrl (6)**
Parts (all 500ms)	44±4	40±7	47±3	47±3	12±2	12±5	8±4	17±2	21±3	20±6	23±4	21±4
Parts (last 200ms)	11±5	11±9	18±3	12±4	22±4	19±8	14±7	30±2	34±5	31±7	36±7	33±6

Table S7: Electrode localization in MNI space (X,Y,Z). See Fig 1 and Supplementary Figure 1 for illustration. LA: left amygdala; RA: right amygdala.

Patient	**NMI coordinates LA**	**NMI coordinates RA**
P17	-22, -2, -24	18, 0, -22
P18	-16, -8, -17	24, -4, -20
P19	-18, -2, -24	21, 2, -22
P20	-18, -10, -16	18, -4, -22
P21	-20, 0, -20	16, -2, -18
P23	-16, 4, -24	16, -4, -22
P25	-21, -5, -25	18, -5, -24
P27	-15, -2, -22	18, -2, -22
P28	-18, -4, -24	20, -4, -24
P29	-18, -6, -18	20, -2, -22

Table S8: Eye movement quantification for the last 200ms before stimulus offset. Shown is the fixation density, conditional on a particular region of the face having been shown. The densities given here are different from those in Table S6, where the fixation density is shown pooled over all trials regardless of which region of the face was shown. P-values are pairwise comparisons between the groups with ASD and their respective controls (Epilepsy-only for neurosurgical patients, normal controls for ASD-only subjects; ± shows s.e.m. over subjects).

	Density left eye ROI [%]				**Density right eye ROI [%]**				**Density mouth ROI [%]**			
Trial Type	**ASD**	**ASD +Epi**	**Epi**	**Ctrl**	**ASD**	**ASD +Epi**	**Epi**	**Ctrl**	**ASD**	**ASD+ Epi**	**Epi**	**Ctrl**
Parts	47±7	44±9	47±4	54±7	50±7	50±9	58±16	50±10	69±12	56±25	43±20	85±5
P value	0.51	0.88			0.97	0.99			0.25	0.64		

Table S9: Behavioral reaction times (RT) for different trial types (eye cutout, mouth cutout, all bubbles). Shown are the average RT (latency to push button from stimulus onset) for all trials of each kind, regardless of whether the response was correct. Means and ±s.e.m. across subjects are given, with n as indicated in brackets in the header row. P-values in the table are pairwise comparisons between the ASD and controls for the ROI shown on the same row. A 2-way ANOVA with factors subject group (ASD, controls) and ROI (eye, mouth) showed no significant main effects nor interactions for all three groups considered (epilepsy during eyetracking, epilepsy during electrophysiology, non-surgical controls), all P>0.2.

	Epilepsy (surgical) group; RT during eye tracking [ms]			Epilepsy (surgical) group; RT during electrophysiology [ms]			Non-Epileptic (non-surgical) group; RT during eye tracking [ms]		
	ASD (2)	**Ctrl (3)**	**p**	**ASD (2)**	**Ctrl (8)**	**p**	**ASD (6)**	**Ctrl (6)**	**p**
Eye cutout	1124±2.4	912±271	0.37	1144±128	976±55	0.22	834±26	775±58	0.45
Mouth cutout	912±41	878±189	0.82	1014±42	991±47	0.82	879±54	790±59	0.29
Bubbles all	974±19	926±132	0.8	1357±346	1032±49	0.28	866±58	815±73	0.60

Table S10: Behavioral reaction times (RT) for different kinds of bubble trials. Shown are the average RT for all trials of each kind, regardless of whether the response was correct, relative to stimulus onset. Means and ±s.e.m. across subjects are given, with n as indicated in brackets in the header row. P-values in the table are pairwise comparisons between the ASD and controls for the ROI shown on the same row. A 2-way ANOVA with factors of subject group (ASD, controls) and ROI (eye, mouth) showed no significant main effects nor interactions for both the surgical and non-surgical group (all P>0.4).

	Epilepsy (surgical) group; RT during eye tracking [ms]			Non-Epileptic (non-surgical) group; RT during eye tracking [ms]		
	ASD (2)	**Ctrl (3)**	**p**	**ASD (6)**	**Ctrl (6)**	**p**
Bubbles – eye only	990±11	923±240	0.74	867±145	816±182	0.60
Bubbles – mouth only	978±20	942±243	0.86	864±146	808±170	0.55
Bubbles – eye and mouth	948±9	900±40	0.81	872±59	789±68	0.38

Supplementary Figure Legends

Figure S1: Individual recording sites in the patients. Sagittal and coronal slices of the MNI152 template MRI scan are shown with electrode positions indicated. The top left shows the position of the coronal slices shown in the other panels. Shown are y=-10, -8, -6, y=-4, y=-2, y=0, and y=2 from left to right. Subjects are marked by colors (compare to Supplementary Table 1 and 7).

Figure S2: Supplemental behavioral results. (A) Nr of bubbles revealed on the last trial, shown on the same scale as in Fig 3C. (B) Average reaction time for each subject for all bubble trials. (A,B) Errorbars are s.e.m. over the datapoints shown. (C,D) Overlay of thresholded (Z>3.5) behavioral classification images on an example face image for the ASD group (a) and controls (b); this figure depicts the same data as does Figure 2d,e.

Figure S3: Single-unit examples. Shown are examples of neurons with significant NCIs from one of the patients with ASD (A) and three controls (B-D). Shown, from top to bottom, are: i) Raster of grouped trials. Bubbles trials are sorted according to overlap of the noise mask with the significant part of the NCI. The overlap is indicated by the magenta line (zero overlap at top, maximal overlap at bottom). Trials are dually aligned to scramble onset (shown for variable amount of time 0.8-1.s) as well as face onset (shown for 500ms). Insets in red show waveforms of the isolated neuron (actual traces in red, clustering waveform in black). ii) peri-stimulus time histogram (PSTH) for the different stimulus categories, iii) PSTH of bubbles trials only, divided into those that overlap with the ROI defined by the NCI and those that do not (inside and outside, respectively). iv) Raw Z-scored NCI (left) and the statistically thresholded NCI superimposed on face (right).

Figure S4: Average 2D Correlation between the independent group BCI from nonsurgical controls and the NCIs of each patient. The correlation was calculated separately for each cell with a significant NCI and then averaged for each patient. (A-F) Correlations for the two

patients with ASD (A,B) and the five controls (C-F). Color code is Z-scores, as determined by bootstrap (see methods). Patient IDs and number of NCIs used for each are as indicated.

Figure S5: Responses to bubbles compared with responses to face cutouts. Results are shown for cells recorded in all 7 patients. Comparison of bubbles response with response to eye/mouth cutouts for all neurons we analyzed (n=91). Cells with NCIs that had more response inside the mouth ROI responded more to the mouth cutouts, resulting in a negative difference between eye and mouth cutouts (n=23, $P<0.05$). Cells with NCIs that responded to one of the eyes responded more to eye cutouts (n=19, $P<0.05$). Cells that did not have an NCI in one of the ROIs had no significant difference (n=49) (although the mean response difference was negative, indicating a higher response for mouth than eye cutouts). * indicates $P<0.05$ when compared to zero.

Figure S6: Eye movements quantified using fixation density maps. Participants saw the same stimuli and performed the same task as during our neuronal recordings while we carried out eye tracking. Data were quantified using fixation density maps that show the probability of fixating different locations. In addition to the entire 500ms period after stimulus onset for bubbles trials (Figure 8, main paper) we also computed the same metric for other trial types and time periods: (A) 500ms period after face onset for eye/mouth parts trials only, (B) 200ms before face offset for bubbles trials, (C) 200ms before face offset for eye/mouth parts only. (D) Shows fixation locations quantified as the conditional probability that a location was fixated, given that it was revealed (shown). This metric (see methods) can only be computed for the bubbles trials. (E-F) Fixation density maps for subsets of cutout trials: left eye (E), right eye (F) and mouth (G) parts only. Density was calculated using the last 200ms before stimulus offset. Subjects only made fixations to the stimuli shown. (A-G) For each row, four separate groups of subjects are shown (from left to right): autism control subjects (n=6), autism subjects with epilepsy (n=2), subjects with only epilepsy (n=3) and neurotypical normal control subjects (n=6).

Supplementary References

Adler, R.J. (1981). The geometry of random fields (New York: Wiley).

Brainard, D.H. (1997). The Psychophysics Toolbox. Spatial Vision 10, 433-436.

Chauvin, A., Worsley, K.J., Schyns, P.G., Arguin, M., and Gosselin, F. (2005). Accurate statistical tests for smooth classification images. J Vision 5, 659-667.

Friston, K.J. (2007). Statistical parametric mapping : the analysis of funtional brain images, 1st edn (Amsterdam ; Boston: Elsevier/Academic Press).

Friston, K.J., Worsley, K.J., Frackowiak, R.S.J., Mazziotta, J.C., and Evans, A.C. (1993). Assessing the significance of focal activations using their spatial extent. Hum Brain Mapp 1, 210-220.

Gosselin, F., and Schyns, P.G. (2001). Bubbles: a technique to reveal the use of information in recognition tasks. Vision Research 41, 2261-2271.

Holt, G.R., Softky, W.R., Koch, C., and Douglas, R.J. (1996). Comparison of discharge variability in vitro and in vivo in cat visual cortex neurons. Journal of neurophysiology 75, 1806-1814.

Jenkinson, M., Beckmann, C.F., Behrens, T.E., Woolrich, M.W., and Smith, S.M. (2012). FSL. Neuroimage 62, 782-790.

Mitchell, J.F., Sundberg, K.A., and Reynolds, J.H. (2007). Differential attention-dependent response modulation across cell classes in macaque visual area V4. Neuron 55, 131-141.

Olsson, P. (2007). Real-time and offline filters for eye tracking. (KTH Royal Institute of Technology).

Rutishauser, U. (2008). Learning and representation of declarative memories by single neurons in the human brain. In Computation&Neural Systems (PhD Thesis) (Pasadena, California Institute of Technology).

Rutishauser, U., Tudusciuc, O., Neumann, D., Mamelak, A.N., Heller, A.C., Ross, I.B., Philpott, L., Sutherling, W.W., and Adolphs, R. (2011). Single-unit responses selective for whole faces in the human amygdala. Curr Biol 21, 1654-1660.

Watson, A.B., and Pelli, D.G. (1983). Quest - a Bayesian Adaptive Psychometric Method. Percept Psychophys 33, 113-120.

Worsley, K.J. (1994). Local Maxima and the Expected Euler Characteristic of Excursion Sets of Chi(2), F and T Fields. Adv Appl Probab 26, 13-42.

Wyler, A.R., Fetz, E.E., and Ward, A.A., Jr. (1975). Firing patterns of epileptic and normal neurons in the chronic alumina focus in undrugged monkeys during different behavioral states. Brain Res 98, 1-20.

SUPPLEMENTAL FIGURE 1

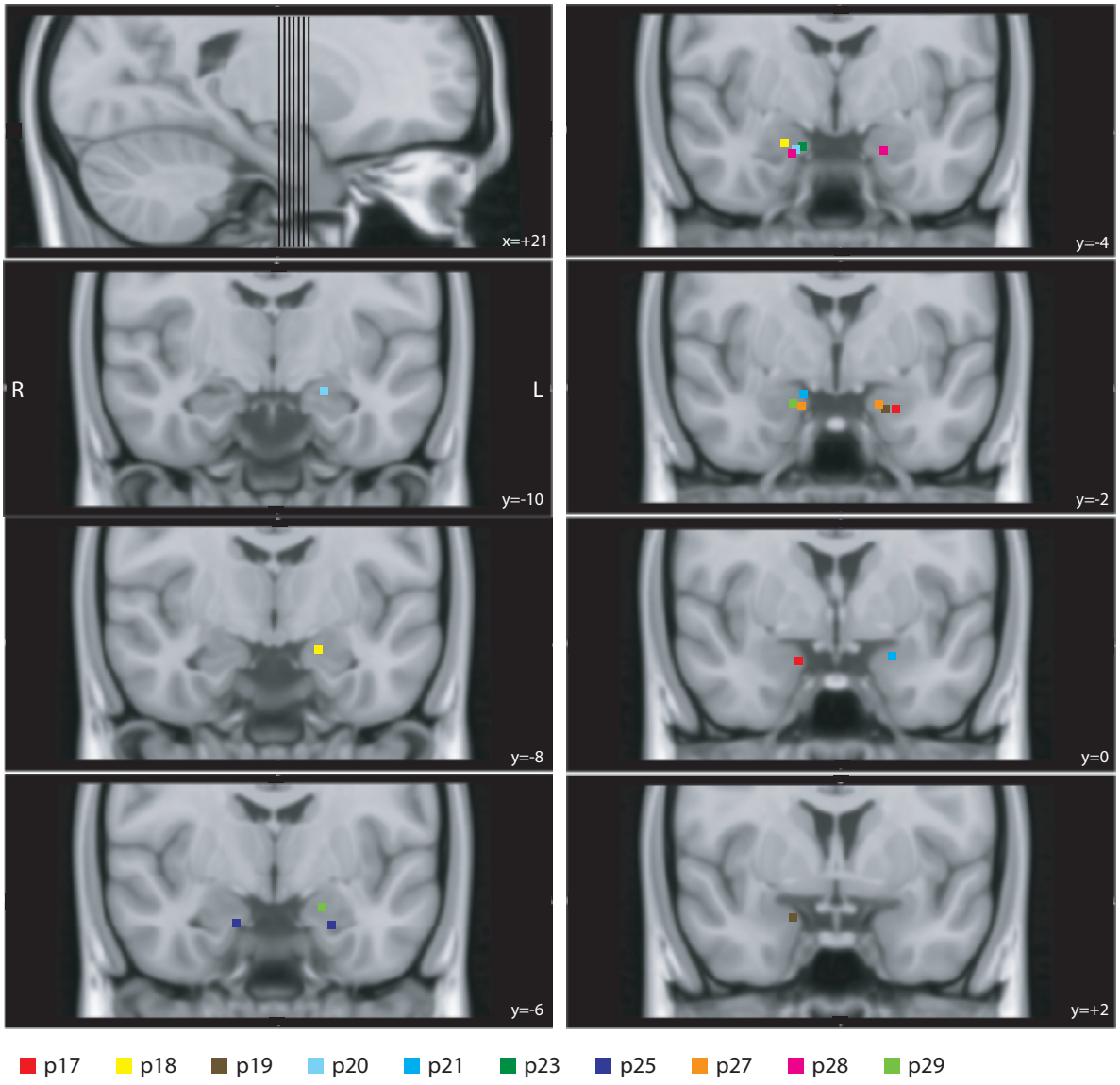

SUPPLEMENTAL FIGURE 2

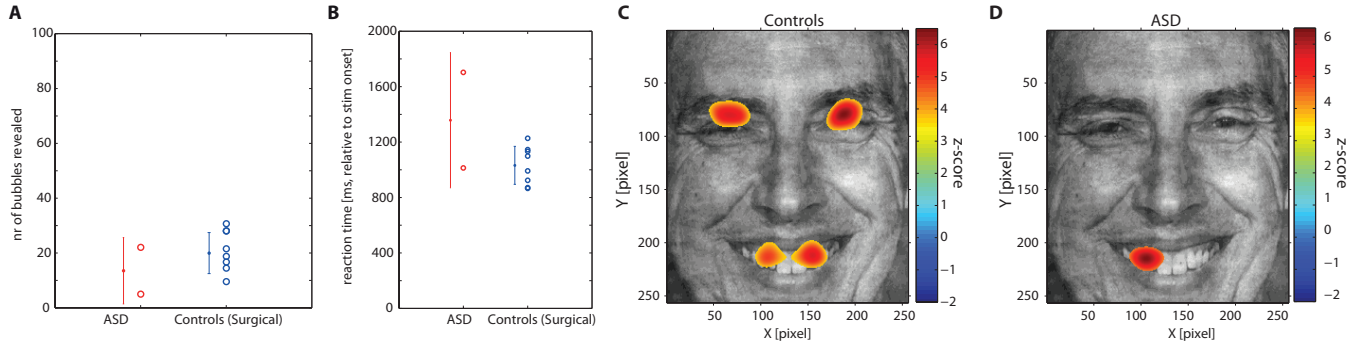

SUPPLEMENTAL FIGURE 3

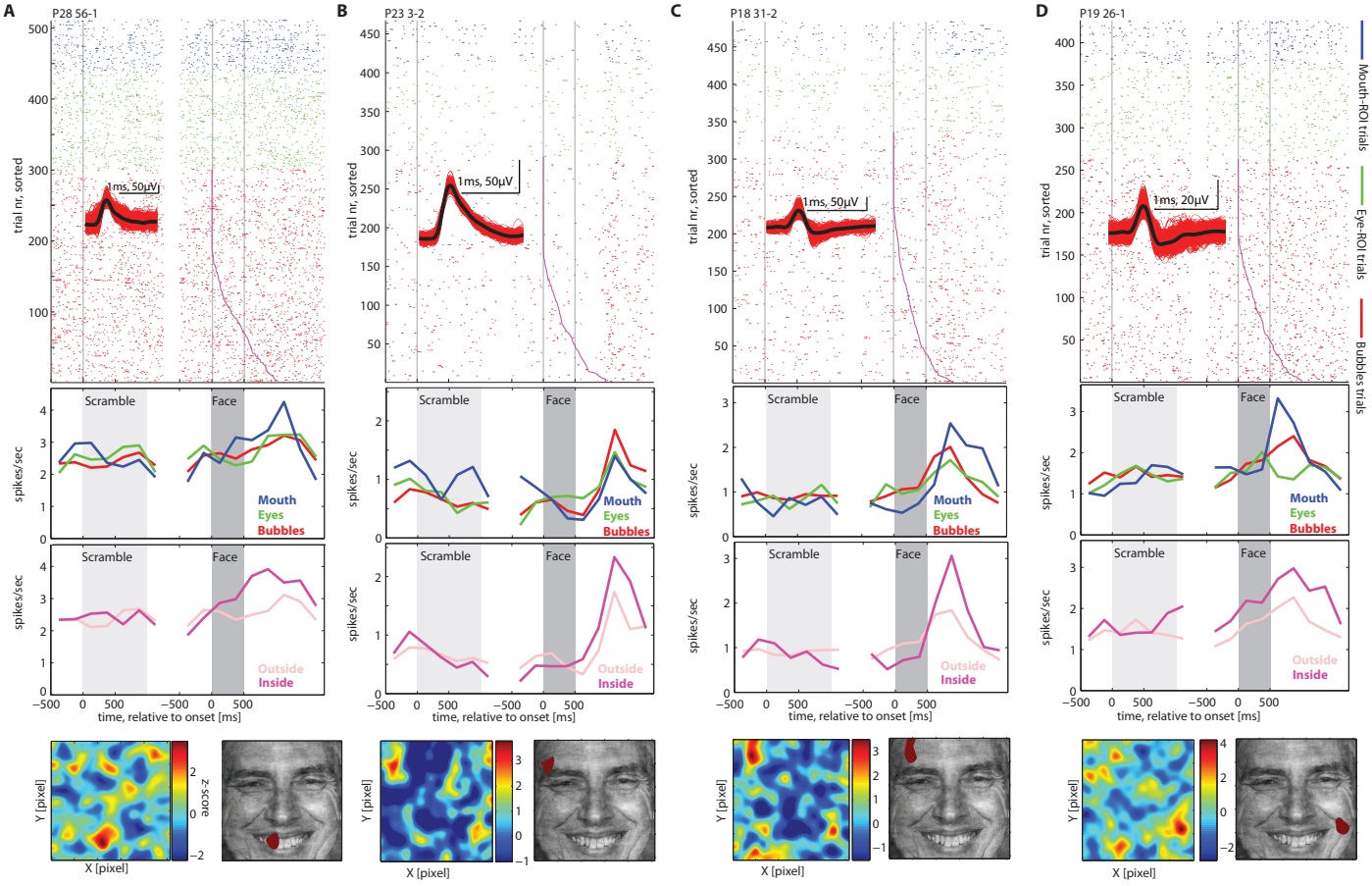

SUPPLEMENTAL FIGURE 4

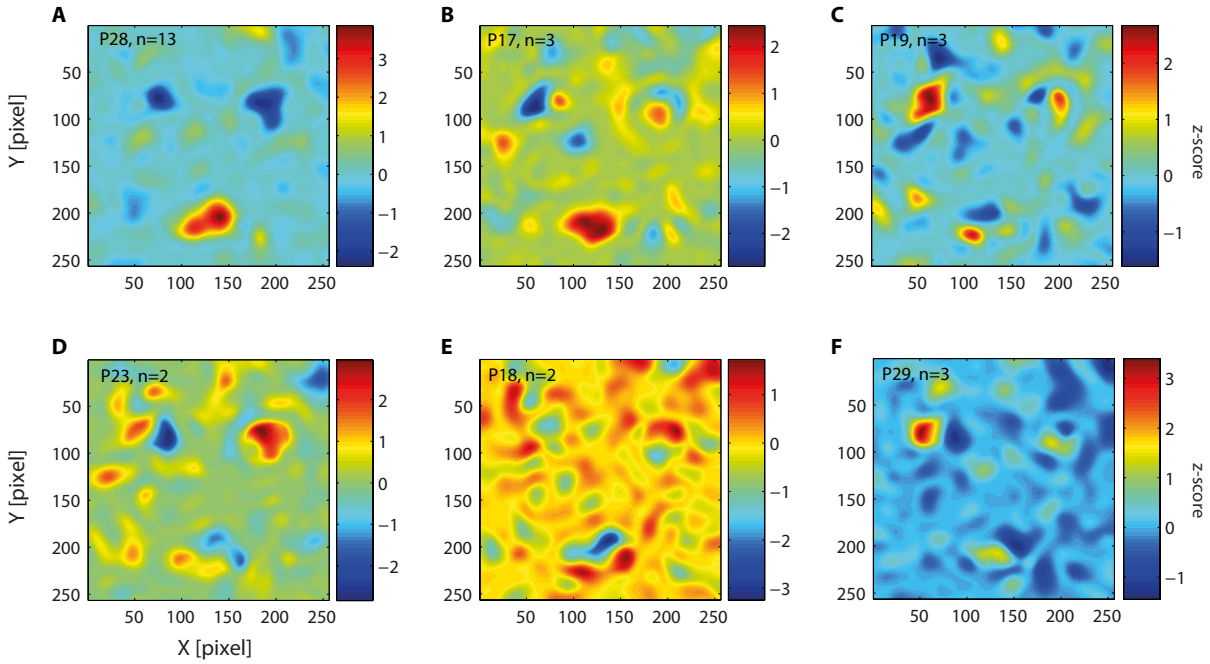

SUPPLEMENTAL FIGURE 5

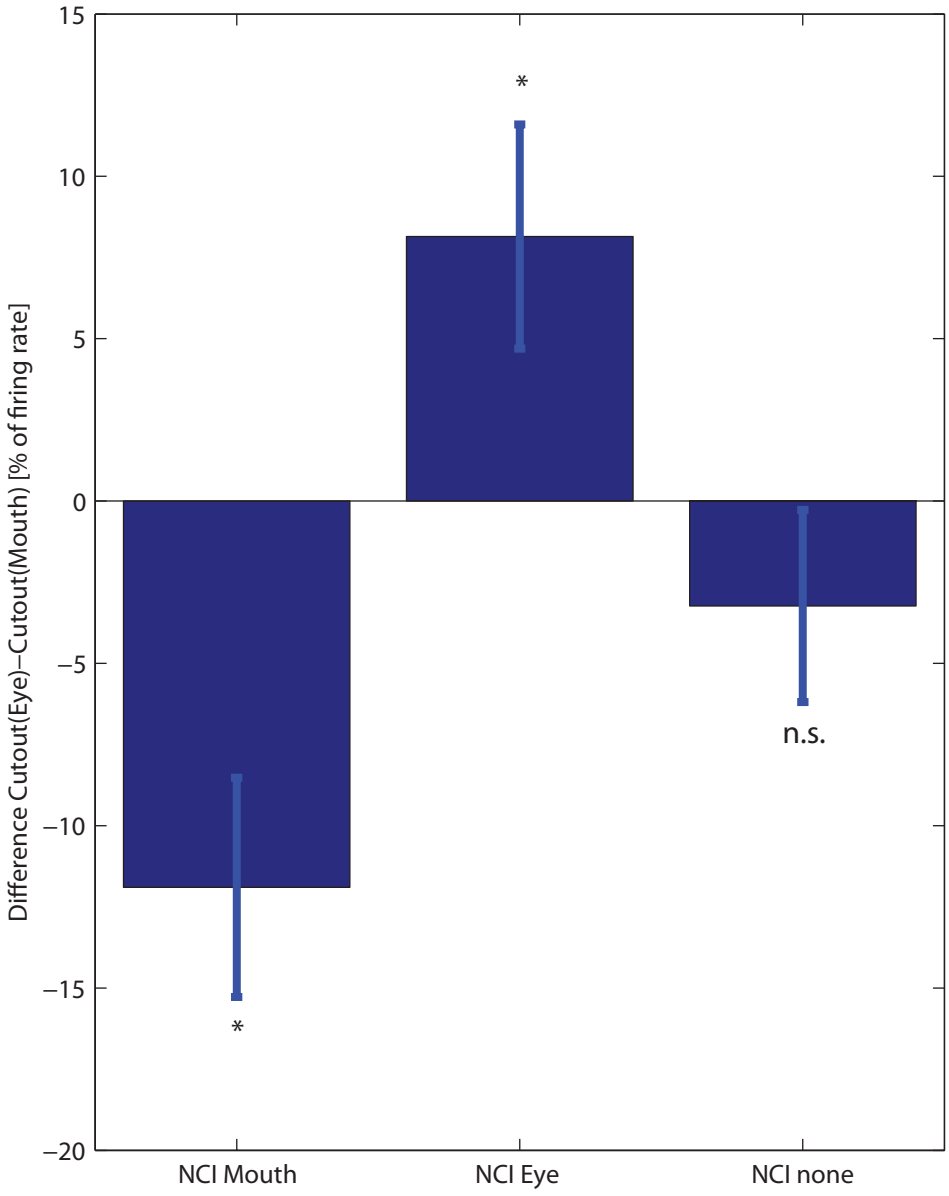

SUPPLEMENTAL FIGURE 6